

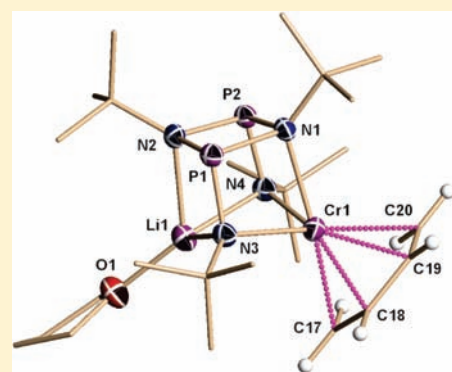
# Vinyl Oxidative Coupling as a Synthetic Route to Catalytically Active Monovalent Chromium

Khalid Albahily,<sup>†</sup> Yacoub Shaikh,<sup>†</sup> Elena Sebastiao,<sup>†</sup> Sandro Gambarotta,<sup>\*,†</sup> Ilia Korobkov,<sup>‡</sup> and Serge I. Gorelsky<sup>†,§</sup>

<sup>†</sup>Department of Chemistry, <sup>‡</sup>X-ray Core Facility, Faculty of Science, and <sup>§</sup>Centre for Catalysis Research and Innovation, University of Ottawa, Ottawa, Ontario K1N 6N5, Canada

**S** Supporting Information

**ABSTRACT:** Reaction of the deprotonated form of *cis*-{(t-Bu)N(H)P[μ-N-(t-Bu)<sub>2</sub>PN(H)(t-Bu)]} with CrCl<sub>3</sub>(THF)<sub>3</sub> afforded the trivalent *cis*-{(t-Bu)NP[μ-N-(t-Bu)<sub>2</sub>PN(H)(t-Bu)]}[Li(THF)]CrCl<sub>2</sub> (**1**). Subsequent reaction with 2 equiv of vinyl Grignard (CH<sub>2</sub>=CH)Mg Cl gave the butadiene derivative (*cis*-{(t-Bu)NP[μ-N-(t-Bu)<sub>2</sub>PN(H)(t-Bu)]}[Li(THF)]Cr(*cis*-η<sup>4</sup>-butadiene) (**3**) formally containing the metal in its monovalent state. The presence of the monovalent state was thereafter confirmed by DFT calculations. The coordination of the butadiene unit appears to be rather robust since reaction with Me<sub>3</sub>P afforded cleavage of the dimeric ligand core but not its displacement. The reaction formed the new butadiene complex [(t-Bu)N–P–N(t-Bu)]Cr(*cis*-η<sup>4</sup>-butadiene)PMe<sub>3</sub> (**4**) containing a regular NPN monoanion. In agreement with the presence of monovalent chromium, complexes **3** and **4** act as single-component self-activating catalysts for selective ethylene trimerization and dimerization, respectively.



## INTRODUCTION

There is a sharp resurgence of interest in the recent literature for the preparation, characterization, and reactivity of monovalent chromium complexes. This interest may be understood in view of the tremendous reactivity of these species capable of forming dinitrogen,<sup>1</sup> inverted sandwich,<sup>2</sup> and the so-called quintupled bonded complexes.<sup>3</sup> There is also a keen industrial interest focused on these complexes since the monovalent state of chromium has been linked to the occurrence of selectivity in the ethylene oligomerization catalytic cycle.<sup>4,5a,5b</sup> Nonetheless, low-valent chromium and its highly coveted monovalent state remain scarce. This is in spite of the existence of a fairly large family of chemically inert carbonyl/arene monovalent derivatives that may be obtained through partial oxidation of readily available zerovalent starting materials.<sup>5</sup> Only recently has an effective strategy been developed to extract the strongly stabilizing carbonyls from the metal coordination sphere, thus enhancing reactivity and catalytic behavior.<sup>5a,b,d</sup>

The utilization of ligands with electron storage capability is a well-consolidated technique to prepare reduced species (low-valent synthons).<sup>6</sup> In other words, it has been possible to prepare complexes with a formal low-valent appearance, in reality possessing higher-valent metals coupled to radical anionic forms of the ligands.<sup>7</sup> Despite the fact that the low-valent appearance is deceptive, the high reactivity expected for genuine low-valent species is remarkably preserved. Chromium falls within this same line of behavior<sup>7s</sup> since this strategy has allowed observing a rare case of dinitrogen fixation as well as partial protonation and cleavage.<sup>1b</sup>

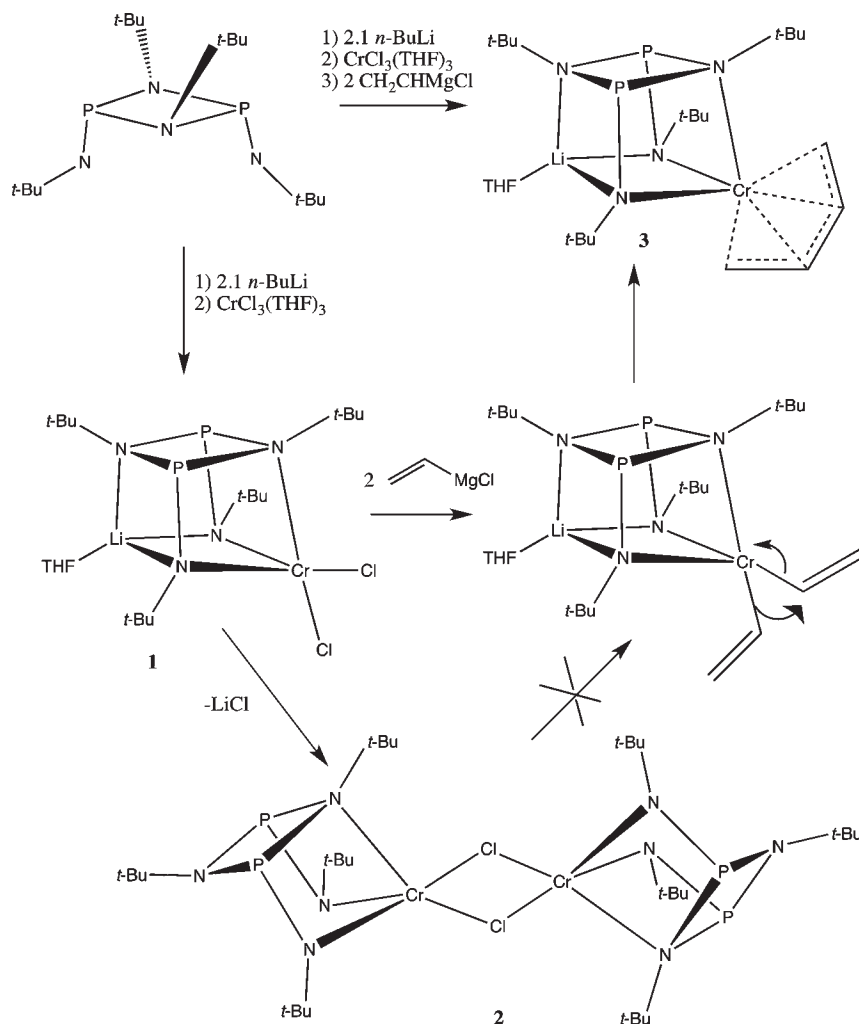
In this work we have explored a synthetic pathway to monovalent chromium alternative to the traditional reductions with alkali metal, hydrides, or alkyl aluminum. In fact, one of the problems to be faced in reaching the monovalent state, especially during catalytic cycles, is the chromium's redox dynamism. In other words, the mono-, di-, and trivalent states readily interconvert, even in the presence of a reducing agent,<sup>4c,8</sup> via disproportionation triggered by intermediate dimeric aggregations. Therefore, all the ligands' features, such as steric hindrance and electron storage capability, which might be capable of preventing clusterification or minimally stabilizing the monovalent state, may be the key to the preparation of monovalent chromium complexes or synthons. Furthermore, due to the generally good stability of chromium's divalent state, it is important to develop two-electron reduction pathways of trivalent precursors capable of bypassing divalent intermediates. A particularly illustrative example is provided by the *in situ* formation of monovalent complexes during the catalytic cycles for selective ethylene tri- and tetramerization. Catalyst activation in those cases relies on the double alkylation of the trivalent center followed by two-electron reductive elimination.<sup>2</sup>

Given this background, we have now probed the possibility of performing a two-electron reduction of trivalent chromium via Stille-type oxidative coupling of two vinyl functions, in line with the behavior of the platinoid metal systems.<sup>9</sup> This methodology

Received: February 1, 2011

Published: April 06, 2011

Scheme 1



stems from the basic idea that a butadiene unit, generated by the oxidative coupling of the two vinyls, could sufficiently stabilize the monovalent state. Of course there was always the possibility that, due to a large extent of back-bonding, the oxidation state might be increased and the oligomerization behavior quenched. In addition, we have recently observed that this reaction carried out on a Cr derivative of an NP<sup>V</sup>N ligand afforded a strange trinuclear complex where three divalent centers were clustered around a doubly deprotonated radical trianion form of butadiene.<sup>10</sup> Taking into consideration all these possibilities, we have attempted now the double vinylation of a trivalent chromium complex formed with an anionic ligand system based on the NP<sup>III</sup>N framework. Previous work from our laboratory has clearly indicated that this ligand is versatile for catalytic purposes, having allowed isolation of rare species and switchable catalytic systems.<sup>11c</sup> Furthermore, there have been a few instances where we have observed that activation with most reducing alkyl aluminum activators, such as Al(*i*-Bu)<sub>3</sub>, resulted in selective trimerization.<sup>11c</sup> This clearly indicates that the monovalent state may be reached and sufficiently stabilized with this ligand.

## RESULTS AND DISCUSSION

The Cr(III) complex starting material was prepared via direct reaction of the deprotonated form of *cis*-{(t-Bu)N(H)P[μ-N

(t-Bu)<sub>2</sub>PN(H)(t-Bu)} with CrCl<sub>3</sub>(THF)<sub>3</sub>. The reaction afforded a new species believed to be the trivalent *cis*-{(t-Bu)NP[μ-N(t-Bu)<sub>2</sub>PN(t-Bu)]}[Li(THF)]CrCl<sub>2</sub> (1) (Scheme 1).

Complex 1 cannot be isolated and normally characterized, since it visibly changes color when its THF solutions are evaporated to dryness and the residue is recrystallized from hexane, or more simply precipitation with nonsolvent was attempted. Its structure is therefore proposed on the basis of the ESI-MS of the reaction solutions and its chemical behavior as highlighted in Scheme 1. In fact, recrystallization from hexane of the dried residues was accompanied by separation of LiCl, affording a new crystalline compound formulated as trivalent (*cis*-{(t-Bu)NP[μ-N(t-Bu)<sub>2</sub>PN(t-Bu)]}CrCl<sub>2</sub>)<sub>2</sub> (2) on the basis of its crystal structure (Figure 1) and analytical data.

The structure of 2 shows a symmetry-generated dimer with the two metal centers, each bearing a N<sub>2</sub>P<sub>2</sub> dianion, bridged by two chlorine atoms in a Cr<sub>2</sub>Cl<sub>2</sub> planar core [Cr(1)–Cl(1) = 2.4094(17) Å, Cr(1)–Cl(1B) = 2.4559(19) Å]. The ligand bonds chromium by using three of its four nitrogen atoms [Cr(1)–N(1) = 1.938(3) Å, Cr(1)–N(2) = 2.071(4) Å] and adopts with chromium an open-cuboid type of structure. The coordination geometry of the metal center may be described in terms of distorted trigonal bipyramidal, with one bridging chlorine

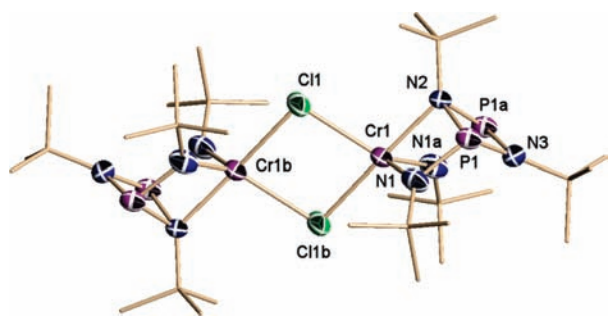


**Figure 1.** Drawing of **2** with thermal ellipsoids at the 50% probability level.

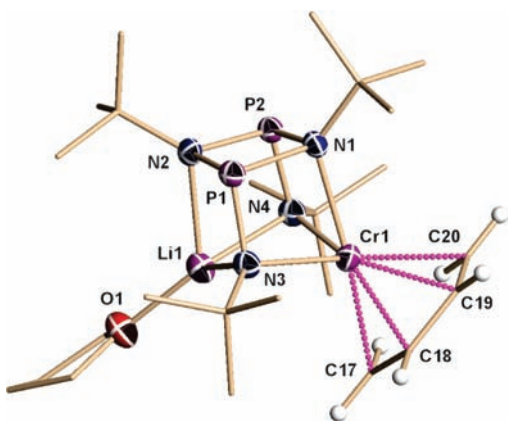


**Figure 2.** Drawing of **3** with thermal ellipsoids at the 50% probability level.

and one nitrogen atom occupying the apical positions [ $N(2A)-Cr(1)-Cl(1) = 169.38(5)^\circ$ ]. The second bridging chlorine and the other two nitrogen donor atoms define the equatorial plane [ $N(1)-Cr(1)-N(2) = 75.22(10)^\circ$ ,  $Cl(1)-Cr(1)-Cl(1B) = 78.06(7)^\circ$ ,  $N(2)-Cr(1)-Cl(1) = 101.47(11)^\circ$ ,  $N(1A)-Cr(1)-N(1) = 108.56(19)^\circ$ ,  $N(1)-Cr(1)-Cl(1) = 112.81(10)^\circ$ ,  $N(1A)-Cr(1)-Cl(1) = 134.62(11)^\circ$ ].

Further support for the structural proposal of **1** is given by the result of its subsequent reaction with vinyl Grignard. Treatment of a THF solution of *in situ* generated **1** with 2 equiv of  $CH_2=CHMgCl$  afforded (*cis*- $\{(t-Bu)NP[\mu-N(t-Bu)]_2PN(t-Bu)\}$ [Li(THF)])Cr(*cis*- $\eta^4$ -butadiene) (**3**), which is the fifth case of a chromium butadiene compound.<sup>12</sup> Even in this case, the structure was elucidated by X-ray diffraction methods showing a monomeric species with the ligand in the same cuboid arrangement proposed for **1** (Figure 2). The retention of lithium in **3** indirectly confirms that the same core structure is likely to be present in **1**.

The structure consists of a chromium atom bonded to one NPN ligand and  $\pi$ -coordinated to one butadiene unit [ $Cr(1)-C(19) = 2.186(3) \text{ \AA}$ ,  $Cr(1)-C(20) = 2.204(4) \text{ \AA}$ ,  $Cr(1)-C(17) = 2.160(3) \text{ \AA}$ ,  $Cr(1)-C(18) = 2.158(4) \text{ \AA}$ ] in *cis* conformation [ $C(17)-C(18) = 1.444(5) \text{ \AA}$ ,  $C(18)-C(19) = 1.402(5) \text{ \AA}$ ,  $C(19)-C(20) = 1.375(6) \text{ \AA}$ ,  $C(18)-C(19)-C(20) = 117.6(4)^\circ$ ,  $C(19)-C(18)-C(17) = 118.3(4)^\circ$ ]. One THF-solvated lithium atom also bonded to the ligand completes the structure [ $Li(1)-O(1) = 1.947(5) \text{ \AA}$ ,  $Li(1)-N(3) = 2.116(5) \text{ \AA}$ ,  $Li(1)-N(4) = 2.126(5) \text{ \AA}$ ,  $Li(1)-N(2) = 2.196(5) \text{ \AA}$ ]. The NPN

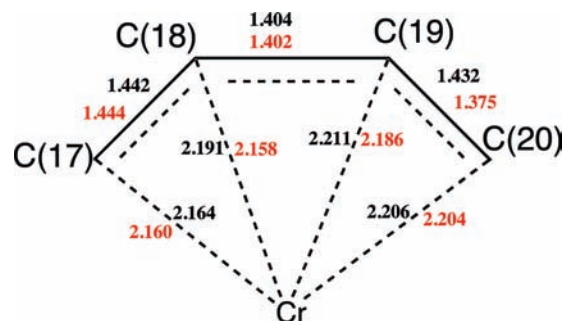


**Figure 3.** Calculated and experimental bond distances for the Cr-butadiene moiety in black and red, respectively.

ligand adopts with both Li and Cr a cuboid type of structure with the two metals located *trans* to each other on one of the cube distorted faces [ $Li(1)-N(3)-Cr(1) = 80.62(15)^\circ$ ,  $Cr(1)-N(4)-Li(1) = 81.39(15)^\circ$ ]. Each metal is bonded to three of the four nitrogen atoms [ $Cr(1)-N(4) = 2.125(2) \text{ \AA}$ ,  $Cr(1)-N(3) = 2.167(2) \text{ \AA}$ ,  $Cr(1)-N(1) = 2.198(2) \text{ \AA}$ ]. The overall coordination around chromium is distorted pseudotetrahedral [ $N(4)-Cr(1)-N(3) = 92.71(8)^\circ$ ,  $N(4)-Cr(1)-N(1) = 72.57(8)^\circ$ ,  $N(3)-Cr(1)-N(1) = 72.43(8)^\circ$ ] considering one coordination site as occupied by the centroid of the  $\pi$ -bonded butadiene unit. All the hydrogen atoms of the coordinated butadiene were located at their expected positions, and the angles of the planar C units were as expected for the  $sp^2$  carbon atoms. However, the C-C distances display a curious asymmetry. One of the two C-C terminal positions is shorter [ $C(19)-C(20) = 1.375(6) \text{ \AA}$ ] than the other [ $C(17)-C(18) = 1.444(5) \text{ \AA}$ ] that is instead in the normal range for a  $\pi$ -coordinated butadiene. However, the thermal parameters of the carbon atoms forming the short distance are somewhat large, showing elongation of the ellipsoids on the C-C vector. This is a possible indication of some minor disorder that could not be modeled by splitting the occupancy. It is therefore conceivable that the short C-C distance may be nothing less than a crystallographic artifact. Furthermore, the asymmetry of bond distances does not significantly affect the Cr-C distances, which are all in the expected range [ $Cr(1)-C(17) = 2.160(3) \text{ \AA}$ ,  $Cr(1)-C(18) = 2.158(4) \text{ \AA}$ ,  $Cr(1)-C(19) = 2.186(3) \text{ \AA}$ ,  $Cr(1)-C(20) = 2.204(4) \text{ \AA}$ ]. Also the angles subtended at the internal carbon atoms are as expected for  $sp^2$  hybrids. All the structural features of the Cr-butadiene moiety compare well with those of the other four existing complexes.<sup>12</sup>

The room temperature magnetic moment of **3** ( $\mu_{\text{eff}} = 3.71 \mu_{\text{MB}}$ ) is in agreement with either high-spin Cr(III) or intermediate-spin Cr(I) electronic configuration with three unpaired electrons. To conclusively clarify the electronic structure of the complex, DFT calculations were undertaken using the atomic coordinates obtained from the crystal structure as a starting geometry. Geometry optimization calculations at the spin-unrestricted PBE level on the full structure of **3** yielded geometrical parameters in excellent agreement with the X-ray values (Figure 3). The calculated C-C distances of the butadiene ligand were  $C(17)-C(18) = 1.442 \text{ \AA}$ ,  $C(18)-C(19) = 1.404 \text{ \AA}$ , and  $C(19)-C(20) = 1.432 \text{ \AA}$ . These values are in the predictable range for butadiene complexes showing a fairly symmetrical bonding mode. DFT calculation predicted a more standard symmetrical bonding mode between the Cr ion and the butadiene ligand. The mismatch between calculated and experimental  $C(19)-C(20)$  distance reiterates that the unusually short experimental value is more

likely an artifact of the large thermal parameters of these two particular C atoms. The predicted Cr–C distances [Cr(1)–C(17) = 2.164 Å, Cr(1)–C(18) = 2.191 Å, Cr(1)–C(19) = 2.211 Å, Cr(1)–C(20) = 2.206 Å] were in excellent agreement with the observed values [Cr(1)–C(17) = 2.160(3) Å, Cr(1)–C(18) = 2.158(4) Å, Cr(1)–C(19) = 2.186(3) Å, Cr(1)–C(20) = 2.204(4) Å]. Among the several possible spin states ( $S = 1/2$ ,  $S = 3/2$ , and  $S = 5/2$ ) that have been used for calculation, the state with three unpaired electrons ( $S = 3/2$ ) yielded the lowest energy and the best agreement between calculated and observed structural parameters, thus lending credibility to the formulation.

The calculated Mayer bond orders for the C–C bonds of the butadiene ligand are 1.11, 1.35, and 1.16 for C(17)–C(18), C(18)–C(19), and C(19)–C(20) bonds, respectively. The net NPA-derived charge and spin densities on the butadiene ligand are  $-0.20$  and  $-0.18$  au, respectively. The three unpaired electrons responsible for the observed magnetism were located in three singly occupied molecular orbitals with 62–68% Cr 3d character, resulting in the spin density of 3.07 for the Cr atom (Figure 4). The NPA-derived atomic charge of the Cr atom ( $+0.15$  au) and NPA-derived populations of the valence orbitals of the Cr atom,  $3d^{4.02} 4s^{0.11} 4p^{0.30}$  for  $\alpha$ -spin orbitals and  $3d^{1.00} 4s^{0.10} 4p^{0.27}$  for  $\beta$ -spin orbitals, are consistent with the Cr(I) description ( $d^5$  electron configuration). Thus, the complex should be considered as containing an intermediate-spin Cr(I) ion.

The formation of the butadiene residue and the two-electron reduction of the metal center is likely to proceed via double vinylation followed by oxidative C–C bond formation (Stille coupling). The trivalent metal center is the recipient of the two electrons necessary to afford the final monovalent chromium complex (Scheme 2). This type of coupling, established for the platinumoid elements,<sup>9a–d</sup> has been observed in only a few cases for the early metals.<sup>9e,f</sup> It is worth noticing that, in the case of a Cr

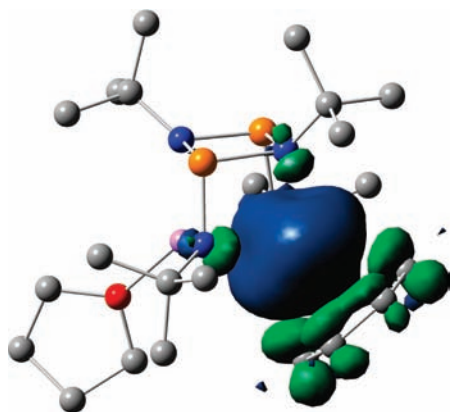
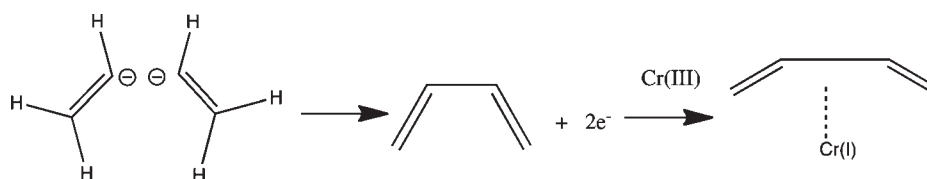


**Figure 4.** Spin density distribution for the ground electronic state of **3** (at PBE/TZVP level). H atoms are not shown for clarity.

## Scheme 2



complex of the NP<sup>V</sup>N ligand system, an identical protocol afforded instead a reduced species with three divalent chromium centers bonded to a doubly deprotonated butadiene radical trianion.<sup>10</sup> In the present case, the transformation is straightforward and provides an easy accessibility to the catalytically relevant monovalent state. The reason for this different behavior is unclear at this stage, and it can be solely attributed to the different oxidation state of the P atom in the two systems. It is not unreasonable to speculate that the presence of a more electron-withdrawing penta-valent P atom might result in an increased acidity of the butadiene unit and consequent easier deprotonation.

Different from all our previous observations,<sup>11</sup> the ligand system has retained its original square-planar dimeric core<sup>12</sup> rather than forming the chelating NPN monoanion, invariably observed in the divalent chromium structures.<sup>11</sup> In an attempt to probe both ligand stability and possible lability of butadiene coordination, we have treated complex **3** with a strongly coordinating ligand such as Me<sub>3</sub>P. The reaction was carried out in hexane, where it gave an instant color change. Two new species could be isolated from the resulting solution via fractional crystallization (Scheme 3). The first complex appeared to be [(*t*-Bu)N–P–N(*t*-Bu)]Cr(*cis*- $\eta^4$ -butadiene)PMe<sub>3</sub> (**4**), as indicated by X-ray crystallography.

The structure (Figure 5) consists of a distorted pseudotetrahedral chromium atom [N(2)–Cr(1)–N(1) = 70.76(15)°, N(2)–Cr(1)–P(2) = 98.78(8)°, N(1)–Cr(1)–P(2) = 98.78(8)°] with one of the coordination sites occupied by the centroid of the  $\pi$ -coordinated butadiene [C(7)–C(8) = 1.404(6) Å, C(8)–C(8A) = 1.373(8) Å, Cr(1)–C(8) = 2.156(3) Å, Cr(1)–C(7) = 2.185(4) Å]. The remaining three coordination sites are occupied by the phosphorus atom of Me<sub>3</sub>P [Cr(1)–P(2) = 2.4348(14) Å] and two nitrogen atoms of the monomeric NPN ligand unit [Cr(1)–N(1) = 2.080(3) Å].

The coordination of Me<sub>3</sub>P during the formation of **4** has resulted in cleavage of the dimeric cuboid form of the ligand and consequent expulsion of a formal monomeric NPN–Li(THF) unit. The robust coordination of phosphine has been clearly the determining factor for the ligand to adopt the monomeric form but not to dissociate butadiene. Accordingly, the second species obtained from the reaction mixture was the lithiated form of the ligand *cis*-{(*t*-Bu)NP[ $\mu$ -N(*t*-Bu)]<sub>2</sub>PN(*t*-Bu)}[Li(THF)]<sub>2</sub> (**5**) where the dimeric core was re-established (Figure 6).

The structure consists of the same cuboid type of structure observed above and with the two lithium atoms, each solvated by one molecule of THF, located on the two opposite corners of one square face of the distorted cube [Li(1)–N(4) = 2.070(5) Å, Li(1)–N(3) = 2.085(5) Å, Li(1)–N(1) = 2.119(6) Å, Li(1)–N(4)–Li(2) = 75.63(18)°, N(4)–Li(1)–N(1) = 76.59(18)°].

The theoretical calculation performed on the geometrical parameters of **3** clearly indicated that the chromium center is

Scheme 3

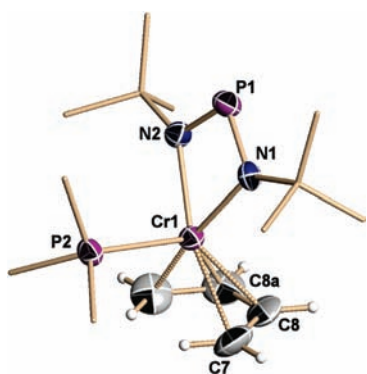
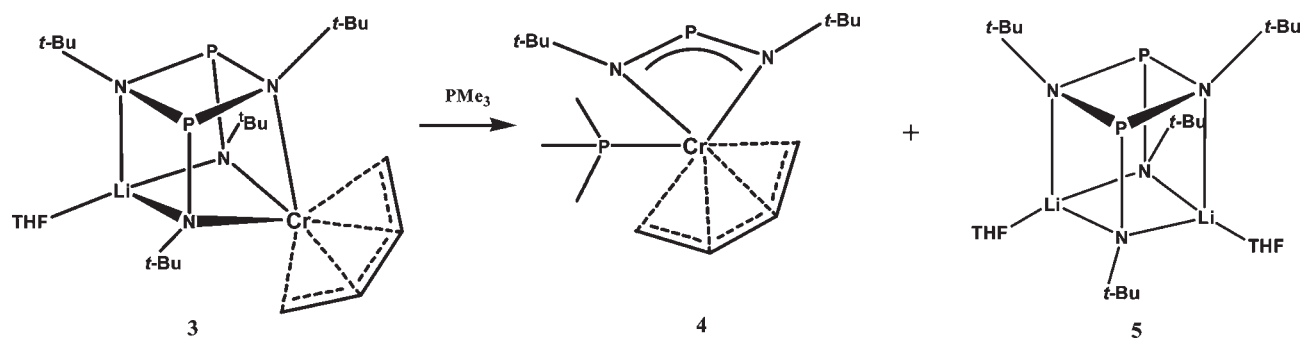


Figure 5. Drawing of 4 with thermal ellipsoids at the 50% probability level.

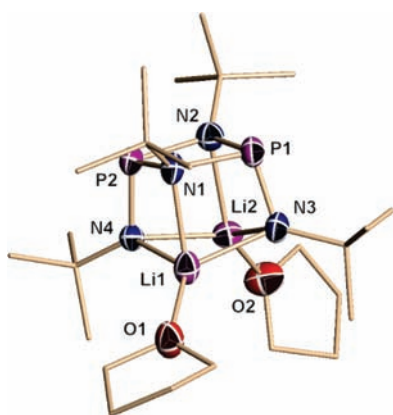


Figure 6. Drawing of 5 with thermal ellipsoids at the 50% probability level.

present in its monovalent state. Accordingly, solutions of **3** in methylcyclohexane, when exposed to 35 bar of ethylene, acted as a self-activating catalytic system of moderate activity producing highly pure 1-hexene and no polymer (Table 1). The reaction also required a rather high temperature and gave only moderate activity. This was rather expected since the initial dissociation of a relatively robust ligand such as butadiene may indeed require a substantial amount of thermal energy. Attempts to activate the complex by using classical alkyl aluminum activators only led to decomposition with the exception of methylaluminumoxane (MAO). In that case, the catalytic activity increased sharply

with a switch to a Schulz–Flory distribution of polymer-free  $\alpha$ -olefins. In turn, this indicates that the alkyl aluminum activator has triggered a disproportionation toward the divalent state.

Complex **2** also displays an interesting behavior since, depending on the reaction conditions, its catalytic performance switched from polymerization to polymer-free oligomerization. In both cases the activities were very high. The choice of the solvent (toluene versus methylcyclohexane) had the most visible effect since polymer-free oligomerization was replaced by good-activity polymerization. Polymer formation could be further increased when  $\text{Me}_3\text{Al}$ -free MAO was used as activator.

The butadiene containing **4** also is a self-activating catalyst producing, however, only 1-butene and not even traces of heavier oligomers or polymer. Selectivity in the formation of 1-butene is commonly observed with nickel-based catalysts, but to the best of our knowledge it has been observed only twice in chromium chemistry.<sup>13</sup> The high selectivity of the present case implies that the presence of coordinated phosphine inhibits the metallacycle ring expansion necessary for the formation of 1-hexene<sup>14</sup> in favor of a reductive elimination. Similar to **3**, the activation with MAO switched the catalytic behavior to a S–F distribution of oligomers.

In conclusion, we have herein reported the double vinylation of a Cr(III) complex affording a genuine monovalent butadiene derivative that is catalytically active. In spite of the robustness of the coordination of the butadiene unit, as apparent from the result of the reaction with phosphine, this complex acts as a single-component selective trimerization catalyst. Should it be possible to labilize the coordination of butadiene by acting on either the substituents on the  $\text{C}_4$  backbone or the nature of this coordinatively versatile ligand, it will be possible to increase the catalytic activity. We find intriguing that complex **4** acts as a single-component dimerization catalyst, implying that phosphine coordination may inhibit metallacycle ring expansion but not its initial formation.

## EXPERIMENTAL SECTION

All reactions were carried out under a dry nitrogen atmosphere. Solvents were dried using an aluminum oxide solvent purification system. Samples for magnetic susceptibility were preweighed inside a drybox equipped with an analytical balance and measured on a Johnson Matthey Magnetic Susceptibility balance. Elemental analyses were carried out with a Perkin-Elmer 2400 CHN analyzer. Data for X-ray crystal structure determination were obtained with a Bruker diffractometer equipped with a 1K Smart CCD area detector. Methylaluminumoxane (MAO, 10% in toluene) was purchased from Aldrich. The ligand

Table 1. Oligomerization Results<sup>a</sup>

catalyst	cocatalyst (equiv)	cocat: +Cr	temp (°C)	alkenes (mL)	PE (g)	activity (g/mmol Cr·h)	C <sub>4</sub> (mol %)	C <sub>6</sub> (mol %)	C <sub>8</sub> (mol %)	C <sub>10</sub> –C <sub>16</sub> (mol %)
2 <sup>b</sup>	MAO	300	60	96	10	2580	3	26	28	43
2 <sup>b</sup>	MAO	1000	60	104	0	2430	2	22	28	48
2 <sup>c</sup>	MAO	1000	60	24	24	1360	1	14	27	58
2 <sup>c</sup>	MAO <sup>d</sup>	1000	60	6	48	1740	0	99	tr	0
2 <sup>c</sup>	MAO <sup>d</sup>	300	60	12	52	2010	0	99	tr	0
2 <sup>c</sup>	MMAO	300	60	8	32	1255	0	99	tr	0
3 <sup>c</sup>	–	–	60	0	0	0	0	0	0	0
3 <sup>c</sup>	–	–	110	2	0	47	0	95	3	2
3 <sup>b</sup>	MAO	500	60	91	0	2125	7	33	24	36
4 <sup>c</sup>	–	–	110	3	0	63	99	0	0	0
4 <sup>b</sup>	MAO	500	60	28	1	690	6	24	26	44

<sup>a</sup> Conditions: Loading 30 μmol of complex, 35 bar of ethylene, reaction time 60 min. <sup>b</sup> 100 mL of toluene. <sup>c</sup> 100 mL of methylcyclohexane. <sup>d</sup> Me<sub>3</sub>Al-free MAO. tr = traces.

*cis*-{(t-Bu)N(H)P[μ-N(t-Bu)]<sub>2</sub>PN(H)(t-Bu)} was prepared according to a published procedure.<sup>15</sup>

**Preparation of *cis*-{(t-Bu)NP[μ-N(t-Bu)]<sub>2</sub>PN(t-Bu)}[Li(THF)]-CrCl<sub>2</sub> (1).** A solution *cis*-{(t-Bu)N(H)P[μ-N(t-Bu)]<sub>2</sub>PN(H)(t-Bu)} (0.348 g, 1 mmol) in THF (10 mL) was treated with *n*-BuLi (0.84 mL, 2.1 mmol, 2.5 M in hexanes). The mixture was allowed to stir at room temperature for 18 h. The resulting solution was added to a suspension of CrCl<sub>3</sub>(THF)<sub>3</sub> (0.375 g, 1 mmol) in THF (5 mL). Stirring was continued at room temperature for 4 h, forming a brown solution. The resulting solution was analyzed by mass spectroscopy. ESI-MS: *m/z* = 548.16 ([M + H]<sup>+</sup>).

**Preparation of *cis*-{(t-Bu)NP[μ-N(t-Bu)]<sub>2</sub>PN(t-Bu)}CrCl<sub>2</sub> (2).** A solution of (t-Bu)(H)NP[μ-N(t-Bu)]<sub>2</sub>PN(H)(t-Bu) (0.240 g, 0.69 mmol) in THF (10 mL) was treated with *n*-BuLi (0.55 mL, 1.38 mmol, 2.5 M in hexanes) and stirred over a 24 h period at room temperature. Solid CrCl<sub>3</sub>(THF)<sub>3</sub> (0.258 g, 0.69 mmol) was added, and the resulting mixture was stirred over 24 h at room temperature. The solvent was then removed *in vacuo* and replaced with hexane (5 mL). The green solution that resulted was centrifuged and the supernatant stored at –30 °C for 4 days, affording deep-green long prisms of 2 (0.191 g, 0.220 mmol 64%),  $\mu_{\text{eff}} = 3.88 \mu_{\text{B}}$ . Crystals spontaneously lose lattice hexane, and samples needed to be pumped *in vacuo* prior to analytical characterization. Anal. Calcd (found) for C<sub>32</sub>H<sub>72</sub>Cl<sub>2</sub>Cr<sub>2</sub>N<sub>8</sub>P<sub>4</sub>: C, 44.29 (44.14); H, 8.36 (8.31); N, 12.91 (12.88). ESI-MS: *m/z* = 867.08 ([M + H]<sup>+</sup>).

**Preparation of *cis*-{(t-Bu)NP[μ-N(t-Bu)]<sub>2</sub>PN(t-Bu)}[Li(THF)]Cr(*cis*-η<sup>4</sup>-butadiene) (3).** A solution of (t-Bu)(H)NP[μ-N(t-Bu)]<sub>2</sub>PN(H)(t-Bu) (0.348 g, 1 mmol) in THF (10 mL) was treated with *n*-BuLi (0.84 mL, 2.1 mmol, 2.5 M in hexanes). The mixture was allowed to stir at room temperature for 20 h. The resulting solution was added to a suspension of CrCl<sub>3</sub>(THF)<sub>3</sub> (0.375 g, 1 mmol) in THF (5 mL). Stirring was continued at room temperature for 2 h. After cooling to –30 °C, a solution of vinylmagnesium chloride (1.28 mL, 1.6 M in THF) was introduced via syringe and the mixture stirred for 18 h at room temperature. The solvent was removed *in vacuo*, and hexane (10 mL) was added. The suspension was centrifuged and, after concentration of the supernatant to 4 mL, stored at –30 °C for 4 days. The resulting crystalline product was filtered, washed with cold hexanes (10 mL), and dried *in vacuo*, affording 3 (0.212 g, 0.40 mmol, 40%) as a brown crystalline solid,  $\mu_{\text{eff}} = 3.81 \mu_{\text{B}}$ . Anal. Calcd (found) for C<sub>24</sub>H<sub>50</sub>CrLiN<sub>4</sub>OP<sub>2</sub>: C, 54.23 (54.24); H, 9.48 (9.46); N, 10.54 (10.53). ESI-MS: *m/z* = 532.58 ([M + H]<sup>+</sup>).

**Preparation of [(t-Bu)N–P–N(t-Bu)]Cr(*cis*-η<sup>4</sup>-butadiene)-PMe<sub>3</sub> (4).** A solution of 3 (0.150 g, 0.28 mmol) in hexane (3 mL) was

treated with PMe<sub>3</sub> (0.016 g, 0.28 mmol) and stirred for 2 days. The resultant dark red-green solution was centrifuged, and slow evaporation of the supernatant yielded dark red-green crystals of 4 (0.031 g, 0.087 mmol, 31%),  $\mu_{\text{eff}} = 3.86 \mu_{\text{B}}$ . Anal. Calcd (found) for C<sub>15</sub>H<sub>33</sub>CrN<sub>2</sub>P<sub>2</sub>: C, 50.70 (50.71); H, 9.36 (9.38); N, 7.88 (7.89). ESI-MS: *m/z* = 356.51 ([M + H]<sup>+</sup>).

**Isolation of *cis*-{(t-Bu)NP[μ-N(t-Bu)]<sub>2</sub>PN(t-Bu)}[Li(THF)]<sub>2</sub> (5).** The insoluble material obtained from the centrifugation of the reaction mixture above was washed using cold hexanes (5 mL) and then dissolved in diethyl ether (2 mL) and stored at –30 °C for 4 days, affording colorless crystals of 5 (0.042 g, 0.083 mmol, 59%). <sup>1</sup>H NMR (C<sub>6</sub>D<sub>6</sub>, 300 MHz, 300 K): δ 1.32 (q, 8H, THF (OCH<sub>2</sub>CH<sub>2</sub>)), 1.48 (s, 18H, C(CH)<sub>3</sub>), 1.55 (s, 18H, C(CH)<sub>3</sub>), 3.67 (t, 8H, THF (OCH<sub>2</sub>CH<sub>2</sub>)). <sup>31</sup>P{<sup>1</sup>H} NMR (C<sub>6</sub>D<sub>6</sub>, 300 MHz, 300 K): δ 160.3 (s). Anal. Calcd (found) for C<sub>24</sub>H<sub>52</sub>Li<sub>2</sub>N<sub>4</sub>O<sub>2</sub>P<sub>2</sub>: C, 57.13 (57.28); H, 10.39 (10.42); N, 11.10 (11.07).

**Oligomerization Results.** Catalytic runs were carried out in 300 mL high-pressure Parr reactors containing a heating/cooling jacket. A preweighed amount of cocatalyst was dissolved in toluene or methylcyclohexane (90 mL) under N<sub>2</sub> prior to loading the reaction vessel. Solutions were heated using a thermostatic bath and charged with ethylene, maintaining the pressure throughout the run. Polymerizations were quenched by releasing the pressure and adding acidified MeOH. When polymers were obtained, they were isolated by filtration, sonicated with an aqueous solution of HCl, rinsed, and thoroughly dried prior to measuring the mass. The reaction mixtures of the oligomerization runs were cooled to –15 °C prior to releasing the overpressure and quenching with acidified MeOH.

**X-ray Crystallography.** Suitable crystals were selected, mounted on a thin, glass fiber with paraffin oil, and cooled to the data collection temperature. Data were collected on a Bruker AXS 1K SMART CCD diffractometer. Data collection was performed with three batch runs at  $\phi = 0.00^\circ$  (600 frames),  $\phi = 120.00^\circ$  (600 frames), and  $\phi = 240.00^\circ$  (600 frames). Initial unit-cell parameters were determined from 60 data frames collected at different sections of the Ewald sphere. Semiempirical absorption corrections based on equivalent reflections were applied. The systematic absences and unit-cell parameters were consistent for the reported space groups. The structures were solved by direct methods, completed with difference Fourier syntheses, and refined with full-matrix least-squares procedures based on *F*<sup>2</sup>. All non-hydrogen atoms were refined with anisotropic displacement parameters. When it was not possible to locate them, the hydrogen atoms were treated as idealized contributions. Complex 2 contains a disordered and partly occupied molecule of hexane in the lattice. All scattering factors and anomalous

Table 2

	2	3	4	5
formula	C <sub>32</sub> H <sub>72</sub> Cl <sub>2</sub> Cr <sub>2</sub> N <sub>8</sub> P <sub>4</sub> (hexane) <sub>0.8</sub>	C <sub>24</sub> H <sub>50</sub> CrLiN <sub>4</sub> OP <sub>2</sub>	C <sub>15</sub> H <sub>33</sub> CrN <sub>2</sub> P <sub>2</sub>	C <sub>24</sub> H <sub>52</sub> Li <sub>2</sub> N <sub>4</sub> O <sub>2</sub> P <sub>2</sub>
M <sub>w</sub>	936.69	531.56	355.37	504.52
space group	monoclinic, C2/m	monoclinic, P2(1)/c	orthorhombic, Pnma	monoclinic, P2(1)/c
a (Å)	24.9305(9)	16.3492(8)	13.5057(6)	10.635(5)
b (Å)	11.2301(4)	9.8141(5)	16.7235(8)	15.822(7)
c (Å)	9.7869(4)	19.5718(10)	8.9182(4)	19.350(8)
α (°)	90	90	90	90
β (°)	109.799(2)	110.647(3)	90	105.545(7)
γ (°)	90	90	90	90
V (Å <sup>3</sup> )	2578.08(17)	2938.6(3)	2014.29(16)	3137(2)
Z	2	4	4	4
radiation	0.71073	0.71073	0.71073	0.71073
T (K)	200(2)	200(2)	200(2)	201(2) K
D <sub>calcd</sub> (g cm <sup>-3</sup> )	1.207	1.201	1.172	1.068
μ <sub>calcd</sub> (mm <sup>-1</sup> )	0.682	0.520	0.721	0.163
F <sub>000</sub>	1004	1148	764	1104
R, R <sub>w</sub> <sup>2a</sup>	0.0717, 0.1849	0.0524, 0.1238	0.0741, 0.1053	0.0521, 0.1287
GoF	1.031	1.029	1.086	1.024

dispersion factors are contained in the SHELXTL 6.12 program library. Relevant crystal data are given in Table 2.

**Computational Details.** DFT calculations were performed using the Gaussian 09 package<sup>16</sup> with the PBE<sup>17</sup> functional and the TZVP<sup>18</sup> basis set. Tight SCF convergence criteria were used for all calculations. Harmonic frequency calculations were performed on the optimized structures to establish the nature of stationary points. The converged wave functions were tested to confirm that they correspond to the ground-state surface. All calculations for the analysis of the electronic structure, including the generation of initial wave functions, Mulliken population analysis,<sup>19</sup> and the calculation of Mayer bond order indices,<sup>20</sup> natural population analysis (NPA)<sup>21</sup>-derived spin densities, and populations of fragment orbitals,<sup>22</sup> were performed using the AOMix software package.<sup>23</sup>

## ■ ASSOCIATED CONTENT

**S Supporting Information.** Complete ref 16 and crystallographic data for the complexes reported in this paper. This material is available free of charge via the Internet at <http://pubs.acs.org>.

## ■ AUTHOR INFORMATION

**Corresponding Author**  
sgambaro@uottawa.ca

## ■ ACKNOWLEDGMENT

This work was supported by the Natural Science and Engineering Research Council of Canada (NSERC). We are grateful to LyondellBasell and Dutch Polymer Institute for partial support.

## ■ REFERENCES

(1) (a) Monillas, W. H.; Yap, G. P. A.; Theopold, K. H. *J. Am. Chem. Soc.* **2007**, *129*, 8090. (b) Vidyaratne, I.; Scott, J.; Gambarotta, S.; Budzelaar, P. *Inorg. Chem.* **2007**, *46*, 7040.

(2) Tsai, Y. C.; Wang, P. Y.; Chen, S. A.; Chen, J. M. *J. Am. Chem. Soc.* **2007**, *129*, 8066.

(3) See, for example: (a) Wagner, F. R.; Noor, A.; Kempe, R. *Nature Chem.* **2009**, *1*, 529. (b) Tsai, Y.-C.; Chen, H.-Z.; Chiang, C.-C.; Yu, J. S. K.; Lee, G. H.; Wang, Y.; Kuo, T. S. *J. Am. Chem. Soc.* **2009**, *131*, 12534. (c) Frenking, G. *Science* **2005**, *310*, 796. (d) Brynda, M.; Gagliardi, L.; Widmark, P. O.; Power, P. P.; Roos, B. O. *Angew. Chem., Int. Ed.* **2006**, *45*, 3804. (e) Nguyen, T.; Sutton, A. D.; Brynda, S.; Fettinger, J. C.; Long, G. J.; Power, P. P. *Science* **2005**, *310*, 844.

(4) See, for example: (a) Jabri, A.; Mason, C. B.; Sim, Y.; Gambarotta, S.; Burchell, T. J.; Duchateau, R. *Angew. Chem., Int. Ed.* **2008**, *47*, 9717. (b) Vidyaratne, I.; Nikiforov, G. B.; Gorelski, S. I.; Gambarotta, S.; Duchateau, R.; Korobkov, I. *Angew. Chem., Int. Ed.* **2009**, *48*, 6522. (c) Licciulli, S.; Thapa, I.; AlBahily, K.; Korobkov, I.; Gambarotta, S.; Duchateau, R.; Chevalier, R.; Schuhen, K. *Angew. Chem., Int. Ed.* **2010**, *49*, 9225. (d) Skobelev, I. Y.; Panchenko, V. N.; Lyakin, O. Y.; Bryliakov, K. P. V.; Zakharov, A.; Talsi, E. P. *Organometallics* **2010**, *29*, 2943.

(5) (a) Bowen, L. E.; Haddow, M. F.; Orpen, A. G.; Wass, D. *Dalton Trans.* **2007**, 1160. (b) Dulai, A.; de Bod, H.; Hanton, M. J.; Smith, D. M.; Downing, S.; Mansell, S. M.; Wass, D. F. *Organometallics* **2009**, *28*, 4613. (c) McGuinness, D. S. *Chem. Rev.* **2011**, *111*, 2321 and references cited therein. (d) Wass, D. *Dalton Trans.* **2007**, 816.

(6) The term “synthon” or “synthetic equivalent” was introduced by Corey and used to define “a structural unit within a molecule related to a possible synthetic operation”. In coordination and organometallic chemistry, it can be also attributed to molecules that behave as synthetic equivalents of species that unlikely exist. (a) Diaconescu, P.; Arnold, P. L.; Baker, T.; Mendiola, D.; Cummins, C. C. *J. Am. Chem. Soc.* **2000**, *122*, 6108. (b) Warner, B. P.; Scott, B. L.; Burns, C. J. *Angew. Chem., Int. Ed.* **1998**, *37*, 959. (c) Fagan, P. J.; Manriquez, J. M.; Marks, T. J.; Day, C. S.; Vollmer, S. H.; Day, V. W. *Organometallics* **1982**, *1*, 170.

(7) See, for example: (a) Wile, B. M.; Trovitch, R. J.; Bart, S. C.; Tondreau, A. M.; Lobkovsky, E.; Milsmann, C.; Bill, E.; Wiegardt, K.; Chirik, P. J. *Inorg. Chem.* **2009**, *48*, 4190. (b) Russell, S. K.; Lobkovsky, E.; Chirik, P. J. *J. Am. Chem. Soc.* **2009**, *131*, 36. (c) Evans, W. J.; Takase, M. K.; Ziller, J. W.; DiPasquale, A. G.; Rheingold, A. L. *Organometallics* **2009**, *28*, 236. (d) Trovitch, R. J.; Lobkovsky, E.; Chirik, P. J. *J. Am. Chem. Soc.* **2008**, *130*, 11631. (e) Scott, J.; Vidyaratne, I.; Korobkov, I.; Gambarotta, S.; Budzelaar, P. H. M. *Inorg. Chem.* **2008**, *47*, 896. (f) Fernandez, I.; Trovitch, R. J.; Lobkovsky, E.; Chirik, P. J. *Organometallics* **2008**, *27*, 109. (g) Vidyaratne, I.; Scott, J.; Gambarotta, S.;

- Budzelaar, P. H. M. *Inorg. Chem.* **2007**, *46*, 7040. (h) Vidyaratne, I.; Scott, J.; Gambarotta, S.; Duchateau, R. *Organometallics* **2007**, *26*, 3201. (i) Bart, S. C.; Chlopek, K.; Bill, E.; Bouwkamp, M. W.; Lobkovsky, E.; Neese, F.; Wieghardt, K.; Chirik, P. J. *J. Am. Chem. Soc.* **2006**, *128*, 13901. (j) Archer, A. M.; Bouwkamp, M. W.; Cortez, M.-P.; Lobkovsky, E.; Chirik, P. J. *Organometallics* **2006**, *25*, 4269. (k) Scott, J.; Gambarotta, S.; Korobkov, I. *Can. J. Chem.* **2005**, *83*, 279. (l) Scott, J.; Gambarotta, S.; Korobkov, I.; Knijnenburg, Q.; De Bruin, B.; Budzelaar, P. H. M. *J. Am. Chem. Soc.* **2005**, *127*, 17204. (m) Sugiyama, H.; Korobkov, I.; Gambarotta, S.; Moeller, A.; Budzelaar, P. H. M. *Inorg. Chem.* **2004**, *43*, 5771. (n) Korobkov, I.; Gambarotta, S.; Yap, G. P. A. *Angew. Chem., Int. Ed.* **2003**, *42*, 4958. (o) Korobkov, I.; Gambarotta, S.; Yap, G. P. A. *Angew. Chem., Int. Ed.* **2003**, *42*, 814. (p) Enright, D.; Gambarotta, S.; Yap, G. P. A.; Budzelaar, P. H. M. *Angew. Chem., Int. Ed.* **2002**, *41*, 3873. (q) Korobkov, I.; Gambarotta, S.; Yap, G. P. A.; Budzelaar, P. H. M. *Organometallics* **2002**, *21*, 3088. (r) Diaconescu, P. L.; Arnold, P. L.; Baker, T. A.; Mindiola, D. J.; Cummins, C. C. *J. Am. Chem. Soc.* **2000**, *122*, 6108. (s) Vidyaratne, I.; Scott, J.; Gambarotta, S.; Duchateau, R. *Organometallics* **2007**, *26*, 3201.
- (8) (a) Thapa, I.; Gambarotta, S.; Duchateau, R.; Kulangara, S. V.; Chevalier, R. *Organometallics* **2010**, *29*, 4080. (b) Temple, C.; Jabri, A.; Crewdson, P.; Gambarotta, S.; Korobkov, I.; Duchateau, R. *Angew. Chem., Int. Ed.* **2006**, *45*, 7050. (c) Albahily, K.; Al-Baldawi, D.; Savard, D.; Gambarotta, S.; Burchell, T. J.; Duchateau, R. *Angew. Chem., Int. Ed.* **2008**, *47*, 5816. (d) Jabri, A.; Crewdson, P.; Gambarotta, S.; Korobkov, I.; Duchateau, R. *Organometallics* **2006**, *25*, 715. (e) Jabri, A.; Temple, C.; Crewdson, P.; Gambarotta, S.; Korobkov, I.; Duchateau, R. *J. Am. Chem. Soc.* **2006**, *128*, 9238.
- (9) (a) Wang, M.; Lin, Z. *Organometallics* **2010**, *29*, 3077 and references cited therein. (b) Alvarez, R.; Faza, O.-N.; de Lera, A. R.; Cardenas, D. J. *Adv. Synth. Catal.* **2007**, *349*, 887 and references cited therein. (c) Terao, J.; Watabe, H.; Kambe, N. *J. Am. Chem. Soc.* **2005**, *127*, 3656. (d) Ananikov, V. P.; Musaev, D. G.; Morokuma, K. *Organometallics* **2001**, *20*, 1652. (e) Beckhaus, R.; Thiele, K.-H. *Z. Anorg. Allg. Chem.* **1989**, *573*, 195. (f) Beckhaus, R.; Thiele, K.-H.; Ströhl, D. *J. Organomet. Chem.* **1989**, *396*, 43.
- (10) Albahily, K.; Fomitcheva, V.; Gambarotta, S.; Korobkov, I.; Murugesu, M.; Gorelski, S. I. *J. Am. Chem. Soc.* **2011**, *133*, DOI: 10.1021/ja200593k.
- (11) (a) Albahily, K.; Al-Baldawi, D.; Gambarotta, S.; Duchateau, R.; Koç, E.; Burchell, T. J. *Organometallics* **2008**, *27*, 22. (b) Albahily, K.; Al-Baldawi, D.; Gambarotta, S.; Duchateau, R.; Koç, E.; Burchell, T. J. *Organometallics* **2008**, *27*, 5943. (c) Albahily, K.; Koç, E.; Al-Baldawi, D.; Savard, D.; Gambarotta, S.; Burchell, T. J.; Duchateau, R. *Angew. Chem., Int. Ed.* **2008**, *47*, 5816.
- (12) (a) Betz, P.; Döhring, A.; Emrich, R.; Goddard, R.; Jolly, P. W.; Kruger, C.; Romao, C. C.; Schönfelder, K. U.; Tsay, Y.-H. *Polyhedron* **1993**, *12*, 2651. (b) Rau, D.; Behrens, U. *Angew. Chem., Int. Ed.* **1991**, *30*, 870. (c) Wang, N. F.; Wink, D. J.; Dewan, J. C. *Organometallics* **1990**, *9*, 335.
- (13) (a) Ackerman, L. J.; Diamond, G. M.; Hall, K. A.; Longmire, J. M.; Micklatcher, M. L. U.S. Patent 2008/0182951 A1. (b) Small, B. L.; Carney, M. J.; Holman, D. M.; O'Rourke, C. E.; Halfen, J. A. *Macromolecules* **2004**, *37*, 4357.
- (14) Agapie, T. *Coord. Chem. Rev.* **2010**, *255*, 861.
- (15) Schranz, I.; Stahl, L. *Inorg. Chem.* **1998**, *37*, 1493.
- (16) Frisch, M. J.; et al. *Gaussian 09*, Revision A.02; Gaussian Inc.: Wallingford, CT, 2009.
- (17) Perdew, J. P.; Burke, K.; Ernzerhof, M. *Phys. Rev. Lett.* **1997**, *78*, 1396.
- (18) Schäfer, A.; Huber, C.; Ahlrichs, R. *J. Chem. Phys.* **1994**, *100*, 5829.
- (19) Mulliken, R. S. *J. Chem. Phys.* **1955**, *23*, 1833.
- (20) Mayer, I. *Int. J. Quantum Chem.* **1986**, *29*, 73.
- (21) Reed, A. E.; Weinstock, R. B.; Weinhold, F. *J. Chem. Phys.* **1985**, *83*, 735.
- (22) Gorelsky, S. I.; Ghosh, S.; Solomon, E. I. *J. Am. Chem. Soc.* **2006**, *128*, 278.
- (23) (a) Gorelsky, S. I. *AOMix – Software for Electronic Structure Analysis*; Centre for Catalysis Research and Innovation, Department of Chemistry, University of Ottawa: Ottawa, ON, 2011; <http://www.sg-chem.net>. (b) Gorelsky, S. I.; Lever, A. B. P. *J. Organomet. Chem.* **2001**, *635*, 187.